Articles

Synthesis, Structure, Photophysical Properties, and Redox Behavior of Cyclometalated Complexes of Iridium(III) with Functionalized 2,2′-Bipyridines

Francesco Neve,*,† Alessandra Crispini,† Sebastiano Campagna,*,‡ and Scolastica Serroni‡

Dipartimento di Chimica, Università della Calabria, I-87030 Arcavacata di Rende (CS), Italy, and Dipartimento di Chimica Inorganica, Chimica Analitica e Chimica Fisica, Università di Messina, via Sperone 31, I-98166 Messina, Italy

Received November 12, 1998

The new functionalized polypyridine ligands 4′-(4-chlorophenyl)-6′-phenyl-2,2′-bipyridine (clpbpy), 4′-(4-tolyl)-6′-phenyl-2,2′-bipyridine (tpbpy), and 4′-(4-carboxyphenyl)-6′-phenyl-2,2′-bipyridine (cpbpy), together with the known 4′-(4-hydroxyphenyl)-6′-phenyl-2,2′-bipyridine (hpbpy) and 4′-(4-tolyl)-2,2′:6′,2″-terpyridine (ttpy) have been used to prepare a new series of Ir(III) cyclometalated compounds $[Ir(ppy)_2(HL\text{-}X)][PF_6]$ (ppy is the monoanion of 2-phenylpyridine; HL-X = hpbpy (**1**), clpbpy (**2**), tpbpy (**3**), cpbpy (**4**), and ttpy (**5**)). All the new species have been characterized by IR and ^{1}H NMR, and the crystal structure of **4** is also presented and discussed. All the metal complexes exhibit oxidation mainly centered on an orbital derived from an Ir−(C^-) σ-bond and ligand-centered reduction processes; all of them are luminescent from ^{3}MLCT levels both at 77 K in a rigid matrix and at 298 K in fluid solution. The redox and absorption properties are more or less insensitive to the remote substituents on the rotationally free 4′-phenyl ring, whereas fine-tuning of the luminescence properties is observed on changing substituents. The results show that the "energy gap law" for radiationless decay in the weak coupling limit is obeyed by this series of complexes, when complex **5** is excluded. Interestingly, the slope of the linear relationship between ln k_{nr} and the emission energy at room temperature is significantly smoother than that reported for other luminescent polypyridine complexes containing different metals. Because of the high luminescence quantum yield and the presence of functionalities in the polypyridine ligand framework, the complexes reported may be considered as useful building blocks for light- and redox-active, multicomponent supramolecular systems.

Introduction

The design of luminescent and redox-active transition metal complexes has been at the center of extensive research efforts during the last fifteen years.[1,2] In particular, systems exhibiting metal-to-ligand charge-transfer (MLCT) luminescence have been investigated because of the key role these systems have played and still play for the understanding of processes of theoretical and potentially applicative interest, such as photoinduced long-range electron and energy transfer, chemiluminescence, and the monitoring of chemical environment.[2,3]

Within the field, very recently MLCT emitters have been extensively used as ideal building blocks for supramolecular systems whose properties and functions can be activated (or exploited) by light.[4] It is now clear from these studies that to optimize the functions of the a supramolecular system, the choice of the metal complexes to be used as chromophores/luminophores is crucial.

Most of the former studies involved Ru(II) and Os(II) polypyridine complexes. Ir(III) cyclometalated species are far less exploited than Ru(II) and Os(II) compounds from this viewpoint, mainly because of synthesis problems. However, owing to their relatively high luminescence quantum yields and their ability to behave as photoreductants,[2d,5−9] it is foreseen that Ir(III) cyclometalated compounds may profitably replace Ru(II) and Os(II) complexes as building blocks for supramolecular systems designed for specific functions. Indeed, examples

* To whom correspondence should be addressed. E-mail: f.neve@unical.it or photochem@chem.unime.it).

† Università della Calabria.

‡ Università di Messina.

(1) (a) *Photochemistry and Photophysics of Coordination Compounds*; Yersin, H., Vogler, A., Eds.; Springer-Verlag: Berlin, 1987. (b) Kalyanasundaram, K. *Photochemistry of Polypyridine and Porphyrin Complexes*; Academic Press: London, 1992. (c) Roundhill, D. M. *Photochemistry and Photophysics of Metal Complexes*; Plenum: New York, 1994.

(2) (a) Meyer, T. J. *Pure Appl. Chem.* **1986**, *58*, 1193. (b) Juris, A.; Balzani, V.; Barigelletti, F.; Campagna, S.; Belser, P.; von Zelewsky, A. *Coord. Chem. Rev.* **1988**, *84*, 85. (c) Meyer, T. J. *Acc. Chem. Res.* **1989**, *22*, 163.(d) Maestri, M.; Balzani, V.; Deuschel-Cornioley, C.; von Zelewsky, A. *Adv. Photochem.* **1992**, *17*, 1. (e) Balzani, V. Juris, A.; Venturi, M.; Campagna, S.; Serroni, S. *Chem. Rev.* **1996**, *96*, 759.

(3) (a) Fox, M. A.; Chanon, M., Eds. *Photoinduced Electron Transfer*; Elsevier: New York, 1988. (b) Scandola, F.; Indelli, M. T.; Chiorboli, C.; Bignozzi, C. A. *Top. Curr. Chem.* **1990**, *158*, 73. (c) Chen, P.; Meyer, T. J. *Chem. Rev.* **1998**, *98*, 1439.

(4) (a) Balzani, V.; Scandola, F. *Supramolecular Photochemistry*; Horwood, Chichester, 1991. (b) Bard, A. J. *Integrated Chemical Systems*; Wiley: New York, 1994. (c) Bignozzi, C. A.; Schoonover, J. R.; Scandola, F. *Prog. Inorg. Chem.* **1997**, *44*, 1. (d) Balzani, V.; Campagna, S.; Denti, G.; Juris, A.; Serroni, S.; Venturi, M. *Acc. Chem. Res.* **1998**, *31*, 26. (e) Flamigni, L.; Barigelletti, F.; Armaroli, N.; Collin, J.-P.; Sauvage, J.-P.; Williams, J. A. G. *Chem. Eur. J.* **1998**, *4*, 1744. (f) Zahavy, E.; Fox, M. A. *Chem. Eur. J.* **1998**, *4*, 1647.

10.1021/ic981308i CCC: $18.00
Published on Web 04/24/1999

of multicomponent (supramolecular) systems based on Ir(III) chromophores have recently been reported.[10,11]

The above reasoning prompted us to design a new series of Ir(III)-based chromophores containing properly functionalized ligands. These chromophores should be suitable for integration into larger multicomponent systems by taking advantage of the functionalities which are present in the ligand structure. As the first step toward this goal, we report here the synthesis of several functionalized polypyridine ligands and of five new Ir(III) cyclometalated derivatives as well as the absorption spectra, luminescence properties (both at room temperature in fluid acetonitrile solution and at 77 K in rigid matrixes), and the redox behavior of the new metal complexes. The ligands investigated in this study (collectively reported thereafter as HL-X) present a bidentate[12] 6′-phenyl-2,2′-bipyridine framework substituted in the 4′-position with a phenyl ring bearing different para X substituents (Scheme 1). The Ir(III) derivatives are of the type $[Ir(ppy)_2(HL\text{-}X)][PF_6]$ (ppy is the monoanion of 2-phenylpyridine; HL-X = hpbpy (**1**), clpbpy (**2**), tpbpy (**3**), and cpbpy (**4**)). The synthesis and characterization of the model species $[Ir(ppy)_2(ttpy)][PF_6]$ (**5**) (where ttpy = 4′-(4-tolyl)-2,2′:6′,2″-terpyridine) is also reported. Structural information on the iridium derivatives **1**−**5** has been obtained by an X-ray diffraction study of complex **4**.

Experimental Section

Materials. Ammonium acetate (Lancaster), ammonium hexafluorophosphate (Fluka), and 1-[2-oxo-2-(phenyl)ethyl]pyridinium bromide (Lancaster) were used as received. Reagent grade solvents from Aldrich were used as supplied. 1-[2-Oxo-2-(2-pyridyl)ethyl]pyridinium iodide[13a] and 1-(2-pyridyl)-3-(phenyl-4-X)propen-1-one (X = Cl, Me, COOH) were prepared following standard procedures.[13b]

Synthesis of the Ligands. Except for the 4′-(4-hydroxyphenyl)-6′-phenyl-2,2′-bipyridine (hpbpy) which was obtained as recently reported by our group,[14] all the 4′-substituted 6′-phenyl-2,2′-bipyridine ligands were prepared from the appropriate enone in a similar manner. The following procedure is for a typical preparation.

Scheme 1

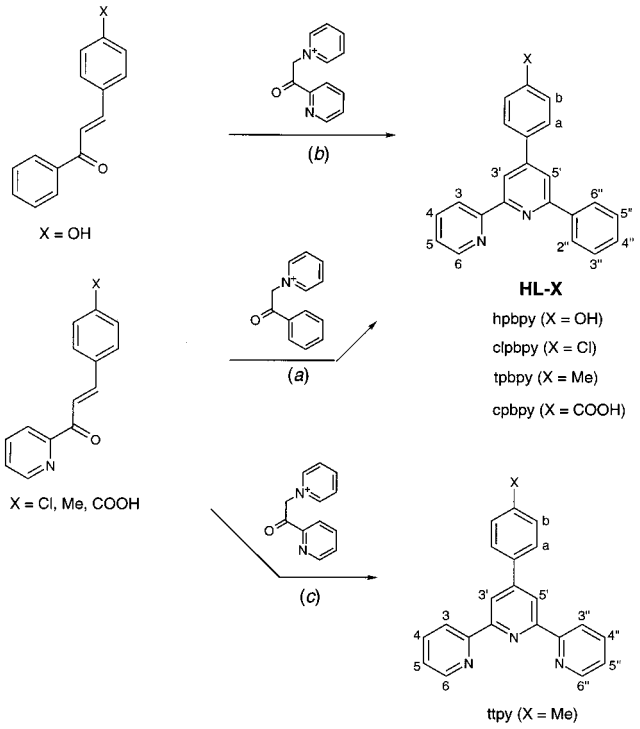

4′-(4-Chlorophenyl)-6′-phenyl-2,2′-bipyridine (clpbpy). An excess of ammonium acetate (approximately 10 equiv) was added to a mixture of 1-(2-pyridyl)-3-(4-chlorophenyl)propen-1-one (0.60 g, 2.46 mmol) and 1-[2-oxo-2-(phenyl)ethyl]pyridinium bromide (0.69 g, 2.46 mmol) in methanol (15 mL). After refluxing for 5−7 h, the reaction mixture was allowed to cool which led to the formation of greenish yellow needles of pure product. The solid was filtered off, washed with cold methanol, and dried under vacuum. A further crop of the desired product was obtained upon reflux of the mother liquor for another 5−6 h and subsequent workup. Overall yield: 63%. Anal. Calcd for $C_{22}H_{15}ClN_2$: C, 77.08; H, 4.41; N, 8.17. Found: C, 76.40; H, 4.31; N, 8.27. ^{1}H NMR ($CDCl_3$): δ (ppm) 8.71 (br d, 1 H, H^6), 8.67 (d, 1 H, H^3, J = 8.0 Hz), 8.59 (d, 1 H, $H^{3'}$, J = 1.5 Hz), 8.18 (m, 2 H, $H^{2'',6''}$), 7.91 (d, 1 H, $H^{5'}$, J = 1.5 Hz), 7.86 (ddd, 1 H, H^4, J = 8.0, 7.5, 1.7 Hz), 7.74 (d, 2 H, H^b, J = 8.3 Hz), 7.56−7.44 (m, 5 H, H^a + $H^{3'',4'',5''}$), 7.34 (ddd, 1 H, H^5, J = 7.5, 5.0, 1.1 Hz).

4′-(4-Tolyl)-6′-phenyl-2,2′-bipyridine (tpbpy). White needles. Yield: 63%. Anal. Calcd for $C_{23}H_{18}N_2$: C, 85.68; H, 5.63; N, 8.69. Found: C, 85.33; H, 5.67; N, 8.90. ^{1}H NMR ($CDCl_3$): δ (ppm) 8.73 (dd, 1 H, H,[6] J = 5.0, 1.6 Hz), 8.69 (d, 1 H, H^3, J = 8.0 Hz), 8.64 (d, 1 H, $H^{3'}$, J = 1.4 Hz), 8.21 (m, 2 H, $H^{2'',6''}$), 7.99 (d, 1 H, $H^{5'}$, J = 1.4 Hz), 7.87 (ddd, 1 H, H^4, J = 8.0, 7.5, 1.8 Hz), 7.75 (d, 2 H, H^b, J = 8.0 Hz), 7.57−7.44 (m, 3 H, $H^{3'',4'',5''}$), 7.37−7.26 (m, 3 H, H^a + H^5), 2.45 (s, 3 H, Me).

4′-(4-Carboxyphenyl)-6′-phenyl-2,2′-bipyridine (cpbpy). Yellowish white needles. Yield (after recrystallization from hot acetic acid): 47%. Anal. Calcd for $C_{23}H_{16}N_2O_2$: C, 78.40; H, 4.60; N, 7.80. Found: C, 77.80; H, 4.47; N, 8.20. IR (KBr, cm^{-1}): ν(COO) 1659. ^{1}H NMR ($CDCl_3$−CD_3OD): δ (ppm) 8.70 (br d, 1 H, H^6), 8.66 (d, 1 H, H^3, J = 8.0 Hz), 8.57 (s, 1 H, $H^{3'}$), 8.25−8.21 (m, 4 H, H^b + $H^{2'',6''}$), 8.13 (s, 1 H, $H^{5'}$), 8.03−7.96 (m, 3 H, H^a + H^4), 7.58−7.46 (m, 4 H, H^5 + $H^{3'',4'',5''}$).

4′-(4-Tolyl)-2,2′:6′,2″-terpyridine (ttpy). Pale green needles of the product were obtained as above when reacting 1-[2-oxo-2-(2-pyridyl)-ethyl]pyridinium iodide (4.68 mmol) and 1-(2-pyridyl)-3-(4-tolyl)-propen-1-one (4.68 mmol) with excess ammonium acetate. Yield: 53%. Anal. Calcd for $C_{22}H_{17}N_3$: C, 81.71; H, 5.30; N, 12.99. Found: C, 81.98; H, 5.20; N, 13.40. ^{1}H NMR ($CDCl_3$): δ (ppm) 8.73 (br s, 4 H, $H^{6,6''}$ + $H^{3',5'}$), 8.67 (d, 2 H, $H^{3,3''}$, J = 7.8 Hz), 7.88 (br t, 2 H, $H^{4,4''}$), 7.82 (d, 2 H, H^b, J = 8.2 Hz), 7.34 (br m, 2 H, $H^{5,5''}$), 7.31 (m, 2 H, H^a, J = 8.2 Hz), 2.43 (s, 3 H, Me).

(5) (a) Ohsawa, Y.; Sprouse, S.; King, K. A.; De Armond, M. K.; Hanck, K. W.; Watts, R. J. *J. Phys. Chem.* **1987**, *91*, 1047. (b) King, K. A.; Watts, R. J. *J. Am. Chem. Soc*. **1987**, *109*, 1589. (c) Garces, F. O.; King, K. A.; Watts, R. J. *Inorg. Chem*. **1988**, *27*, 3464. (d) Garces, F. O.; King, K. A.; Watts, R. J. *Inorg. Chem.* **1990**, *29*, 582. (e) Djurovich, P. I.; Watts, R. J. *Inorg. Chem.* **1993**, *32*, 4681. (f) Schmid, B.; Garces, F. O.; Watts, R. J. *Inorg. Chem.* **1994**, *33*, 9.
(6) (a) van Diemen, J. H.; Haasnoot, J. G.; Hage, R.; Müller, E.; Reedijk, J. *Inorg. Chim. Acta*, **1991**, *181*, 245. (b) van Diemen, J. H.; Hage, R.; Lempers, H. E. B.; Reedijk, J.; Vos, J. G.; De Cola, L.; Barigelletti, F.; Balzani, V. *Inorg. Chem.* **1992**, *31*, 3518.
(7) Calogero, G.; Giuffrida, G.; Serroni, S.; Ricevuto, V.; Campagna, S. *Inorg. Chem.* **1995**, *34*, 541.
(8) (a) Didier, P.; Jacquet, L.; Kirsch-DeMesmaeker, A.; Heuber, R.; van Dorsselaer, A. J. *Inorg. Chem.* **1992**, *31*, 4803. (b) Didier, P.; Ortmans, L.; Kirsch-DeMesmaeker, A.; Watts, R. J. *Inorg. Chem.* **1993**, *32*, 5239.
(9) (a) Colombo, M. G.; Hauser, A.; Güdel, H. U. *Inorg. Chem.* **1993**, *32*, 3088. (b) Colombo, M. G.; Brunold, T. C.; Riedner, T.; Güdel, H. U.; Förtsch, M.; Bürgi, H.-B. *Inorg. Chem.* **1994**, *33*, 545. (c) Colombo, M. G.; Hauser, A.; Güdel, H. U. *Top. Curr. Chem.* **1994**, *171*, 143.
(10) Serroni, S.; Juris, A.; Campagna, Venturi, M.; Denti, G.; Balzani, V. *J. Am. Chem. Soc.* **1994**, *116*, 9086.
(11) Molnar, S. M.; Nallas, G.; Bridgewater, J. S.; Brewer, K. J. *J. Am. Chem. Soc.* **1994**, *116*, 5206.
(12) This is also a potentially tridentate donor set as metalation at the 6′-phenyl ring can occur. For examples of such a possibility, see: (a) Neve, F.; Ghedini, M.; Crispini, A. *Chem. Commun.* **1996**, 2463. (b) Neve, F.; Crispini, A.; Campagna, S. *Inorg. Chem.* **1997**, *36*, 6150.
(13) (a) Treffert-Ziemelis, S. M.; Golus, J.; Strommen, D.; Kincaid, J. R. *Inorg. Chem.* **1993**, *32*, 3890. (b) Whittle, B.; Everest, N. S.; Howard, C.; Ward, M. D. *Inorg. Chem.* **1995**, *34*, 2025.
(14) Neve, F., Ghedini, M.; Francescangeli, O.; Campagna, S. *Liq. Cryst.* **1998**, *24*, 673.

Syntheses of the Complexes. All the complexes were prepared from the precursor $[Ir(ppy)_2Cl]_2$[15] using the same synthetic procedure. Therefore, details of the typical procedure are given only once.

$[Ir(ppy)_2(hpbpy)][PF_6]$ (1). A solution of $[Ir(ppy)_2Cl]_2$ (83 mg, 0.077 mmol) in methanol (10 mL) was added to a stirred suspension of the hpbpy ligand (50 mg, 0.154 mmol) in dichloromethane (8 mL). Heating under reflux conditions for 2 h led the starting suspension to become a clear orange solution. After this solution cooled to room temperature, a saturated solution of $[NH_4][PF_6]$ in methanol (2 mL) was added and stirring continued for another 30 min. Partial evaporation of the solvents under reduced pressure afforded an orange, microcrystalline precipitate. The solid was collected on a glass filter frit, washed with diethyl ether, and vacuum-dried to give 134 mg of the product (yield: 90%). Anal. Calcd for $C_{44}H_{32}F_6IrN_4OP$: C, 54.50; H, 3.33; N, 5.78. Found: C, 55.21; H, 3.32; N, 6.11. IR (KBr, cm^{-1}): ν(OH) 3503, ν(PF) 844. ^1H NMR ($CDCl_3-CD_3CN$): δ (ppm) 8.73 (br s, 1 H, $H^{3'}$), 8.66 (d, 1 H, H^3, $J = 8.0$ Hz), 8.18 (br t, 1 H, H^4), 7.96−7.91 (m, 4 H), 7.88 (d, 2 H, H^a, $J = 8.4$ Hz), 7.84 (br t, 1 H), 7.79 (d, 1 H, $J = 5.8$ Hz), 7.70 (br s, 1 H, $H^{5'}$), 7.66 (d, 1 H, $J = 5.8$ Hz), 7.61 (d, 1 H, $J = 8.0$ Hz), 7.47 (m, 1 H, H^5), 7.31 (d, 1 H, $J = 7.7$ Hz), 7.18−7.06 (m, 4 H), 6.99 (t, 2 H, $J = 7.4$ Hz), 6.86 (t, 2 H, $J = 7.5$ Hz), 6.80 (t, 2 H, $J = 7.5$ Hz), 6.63 (t, 3 H, $J = 7.4$ Hz), 6.42 (t, 1 H, $J = 7.4$ Hz), 6.01 (d, 1 H, $J = 7.5$ Hz), 5.62 (d, 1 H, $J = 7.6$ Hz).

$[Ir(ppy)_2(clpbpy)][PF_6]$ (2). Dark yellow solid. Yield: 86%. Anal. Calcd for $C_{44}H_{31}ClF_6IrN_4P$: C, 53.47; H, 3.16; N, 5.67. Found: C, 53.03; H, 3.05; N, 5.75. IR (KBr, cm^{-1}): ν(PF) 847. ^1H NMR (CD_3CN): δ (ppm) 8.77 (br s, 1 H, $H^{3'}$), 8.72 (d, 1 H, H^3, $J = 8.2$ Hz), 8.15 (br t, 1 H, H^4), 8.00−7.79 (m, 8 H), 7.74 (br s, 1 H, $H^{5'}$), 7.68−7.59 (m, 4 H), 7.45 (m, 1 H, H^5), 7.30 (d, 1 H, $J = 7.8$ Hz), 7.15−7.06 (m, 2 H), 6.94 (m, 2 H), 6.82 (t, 1 H, $J = 7.4$ Hz), 6.76 (t, 2 H, $J = 7.8$ Hz), 6.64 (vbr s, 2 H), 6.57 (t, 1 H, $J = 7.4$ Hz), 6.36 (t, 1 H, $J = 7.8$ Hz), 5.96 (d, 1 H, $J = 7.4$ Hz), 5.57 (d, 1 H, $J = 7.5$ Hz).

$[Ir(ppy)_2(tpbpy)][PF_6]$ (3). Dark yellow solid. Yield: 96%. Anal. Calcd for $C_{45}H_{34}F_6IrN_4P$: C, 55.84; H, 3.54; N, 5.79. Found: C, 55.26; H, 3.41; N, 5.61. IR (KBr, cm^{-1}): ν(PF) 847. ^1H NMR (CD_3CN): δ (ppm) 8.78 (d, 1 H, $H^{3'}$, $J = 2.0$ Hz), 8.73 (d, 1 H, H^3, $J = 8.0$ Hz), 8.14 (br t, 1 H, H^4), 7.97−7.80 (m, 8 H), 7.74 (br s, 1 H, $H^{5'}$), 7.67 (d, 1 H, $J = 5.7$ Hz), 7.60 (d, 1 H, $J = 7.5$ Hz), 7.46−7.42 (m, 3 H), 7.30 (d, 1 H, $J = 7.4$ Hz), 7.15−7.06 (m, 2 H), 6.84 (t, 1 H, $J = 7.5$ Hz), 6.75 (t, 2 H, $J = 7.5$ Hz), 6.63 (vbr s, 2 H), 6.56 (t, 1 H, $J = 7.4$ Hz), 6.36 (t, 1 H, $J = 7.3$ Hz), 5.95 (d, 1 H, $J = 7.3$ Hz), 5.57 (d, 1 H, $J = 7.5$ Hz), 2.45 (s, 3 H, Me).

$[Ir(ppy)_2(cpbpy)][PF_6]$ (4). Orange solid. Yield: 72%. Anal. Calcd for $C_{45}H_{32}F_6IrN_4O_2P$: C, 54.11; H, 3.23; N, 5.61. Found: C, 53.95; H, 3.23; N, 5.60. IR (KBr, cm^{-1}): ν(COOH) 2660, 2543, ν(CO) 1721, 1692, ν(PF) 847. ^1H NMR (CD_3CN): δ (ppm) 8.87 (br s, 1 H, $H^{3'}$), 8.78 (d, 1 H, H^3, $J = 8.1$ Hz), 8.25 (d, 2 H, H^b, $J = 8.1$ Hz), 8.19 (br t, 1 H, H^4), 8.12 (d, 2 H, H^a, $J = 8.1$ Hz), 7.98 (m, 3 H), 7.93 (d, 1 H, $J = 5.4$ Hz), 7.88 (m, 2 H), 7.83 (br s, 1 H, $H^{5'}$), 7.71 (d, 1 H, $J = 5.8$ Hz), 7.65 (d, 1 H, $J = 7.7$ Hz), 7.50 (m, 1 H, H^5), 7.34 (d, 1 H, $J = 7.6$ Hz), 6.80 (t, 2 H, $J = 7.5$ Hz), 6.68 (vbr s, 2 H), 6.61 (t, 1 H, $J = 7.5$ Hz), 6.41 (t, 1 H, $J = 7.4$ Hz), 6.00 (d, 1 H, $J = 7.5$ Hz), 5.61 (d, 1 H, $J = 7.7$ Hz).

$[Ir(ppy)_2(ttpy)][PF_6]$ (5). Greenish yellow solid. Yield: 91%. Anal. Calcd for $C_{44}H_{33}F_6IrN_5P$: C, 54.54; H, 343; N, 7.23. Found: C, 54.01; H, 3.37; N, 7.67.. IR (KBr, cm^{-1}): ν(PF) 847. ^1H NMR (CD_3CN): δ (ppm) 8.77 (vbr s, 1 H, H^6), 8.73 (s, 1 H, $H^{3'}$), 8.71 (d, 1 H, H^3, $J = 8.0$ Hz), 8.17 (m, 2 H), 7.96−7.78 (m, 7 H), 7.67 (s, 1 H, $H^{5'}$), 7.63 (d, 1 H, $J = 8.0$), 7.48 (m, 1 H, H^5), 7.44−7.34 (m, 4 H), 7.18−7.10 (m, 2 H), 7.00−6.91 (m, 3 H), 6.75 (t, 1 H, $J = 7.5$ Hz), 6.61 (br t, 2 H), 6.31 (t, 1 H, $J = 7.3$ Hz), 5.87 (d, 1 H, $J = 7.7$ Hz), 5.45 (d, 1 H, $J = 7.5$ Hz), 2.45 (s, 3 H, Me).

Measurements. The ^1H NMR spectra were recorded at 300.13 MHz with a Bruker AC 300 spectrometer; chemical shifts are referenced to internal $SiMe_4$. Infrared spectra were recorded on a Perkin-Elmer 2000 FT-IR spectrophotometer for KBr pellets. Elemental analyses were performed using a Perkin-Elmer 2400 microanalyzer. Electrochemical measurements were carried out in argon-purged acetonitrile at room temperature with a PAR 273 multipurpose equipment interfaced to a PC. The working electrode was a glassy carbon (8 mm^2, Amel) electrode. The counter electrode was a Pt wire, and the reference electrode was an SCE separated with a fine glass frit. The concentration of the complexes was about 5×10^{-4} M. Tetrabutylammonium hexafluorophosphate was used as supporting electrolyte and its concentration was 0.05 M. Cyclic voltammograms were obtained at scan rates of 20, 50, 200, and 500 mV/s. For reversible processes, half-wave potentials (vs SCE) were calculated as the average of the cathodic and anodic peaks. The criteria for reversibility were the separation between cathodic and anodic peaks, the close-to-unity ratio of the intensities of the cathodic and anodic currents, and the constancy of the peak potential on changing scan rate. For irreversible processes, the values reported in Table 4 are the peaks estimated by differential pulse voltammetry (DPV). The number of exchanged electrons was measured with differential pulse voltammetry (DPV) experiments performed with a scan rate of 20 mV/s, a pulse height of 75 mV, and a duration of 40 ms. Experimental error on the redox potentials, ±10 mV. Absorption spectra were recorded with a Kontron Uvikon 860 spectrophotometer. Luminescence spectra were performed with a Perkin-Elmer LS-5B spectrofluorimeter equipped with a Hamamatsu R928 photomultiplier and were corrected for photomultiplier response by using a standard lamp. Emission lifetimes were measured with an Edinburgh FL-900 single-photon counting equipment (nitrogen discharge; pulse width, 3 ns). Emission quantum yields were measured at room temperature (20 °C) with the optically dilute method,[16] calibrating the spectrofluorimeter with a standard lamp. $[Ru(bpy)_3]^{2+}$ in aerated aqueous solution was used as a quantum yield standard, assuming a value of 0.028.[17]

Table 1. Crystallographic Parameters, Collection Data, and Refinement Results for $[Ir(ppy)_2(cpbpy)]PF_6 \cdot 2CH_2Cl_2$ (**4**)

empirical formula	$C_{45}H_{32}F_6N_4O_2PIr \cdot 2CH_2Cl_2$
fw	1167.8
cryst syst	monoclinic
space group	$P2_1/c$
a, Å	11.621(8)
b, Å	27.73(3)
c, Å	15.239(12)
β (deg)	110.62(6)
V, Å^3	4597(5)
Z	4
D_{calc}, g/cm^3	1.687
temp, K	298
wavelength, Å	0.710 73
F(000)	2304
scan type	ω
transm factors	0.188−0.371
no. of indep reflcns	7219 [R(int) = 0.071]
no. of observed reflcns	5817 with $I > 2\sigma(I)$
absorption correction	semiempirical
no. of refined params	556
final R indices[a,b]	$R = 0.0696$, $R' = 0.0824$
g in $w^{-1} = \sigma^2(\|F\|) + g\|F\|^2$	0.0072
goodness-of-fit	1.27
largest and mean Δ/σ	0.193, 0.011

[a] $R = \sum||F_o| - |F_c||/\sum|F_o|$. [b] $R' = [\sum w(|F_o| - |F_c|)^2/\sum w|F_o|^2]^{1/2}$.

X-ray Crystal Structure of $[Ir(ppy)_2(cpbpy)][PF_6] \cdot 2CH_2Cl_2$ (4). Crystals of $[Ir(ppy)_2(cpbpy)][PF_6]$ (**4**) were obtained by slow diffusion of CH_3OH into a saturated CH_2Cl_2 solution of the complex. A single-crystal suitable for X-ray analysis with dimension of 0.40 × 0.60 × 0.50 mm was attached with epoxy adhesive to a glass fiber. Diffraction data were measured on a Siemens R3m/V four-circle diffractometer with an $\omega-2\theta$ scan method using graphite-monochromated Mo Kα radiation. Crystallographic data and refinement parameters are summarized in Table 1. The lattice constants were determined by a least-squares fit of 20 reflections in the range $17.9° < 2\theta > 30.3°$. Two standard reflections ($\bar{4}25$, $5\bar{6}\bar{4}$) were monitored every 98 reflections and showed no systematic variation. All data reduction, including

(15) Sprouse, S.; King, K. A.; Spellane, P. J.; Watts, R. J. *J. Am. Chem. Soc.* **1984**, *106*, 6647.
(16) Demas, J. N.; Crosby, G. A. *J. Phys. Chem.* **1971**, *75*, 991.
(17) Nakamaru, K. *Bull. Chem. Soc. Jpn.* **1982**, *55*, 2697.

Lorentz, polarization, and absorption corrections, structure solution, and refinement were performed using Shelxtl plus software.[18] Atomic scattering factors and anomalous dispersion terms were those supplied in the Siemens structure determination package. Empirical absorption correction, based on ψ scan data[19] was applied. Following the data reduction, 7219 unique reflections remained with 5817 (having $I > 2\sigma(I)$) retained for structure solution and refinement. The structure was solved by standard heavy-atom methods, which allowed the location of the Ir atom, followed by difference Fourier synthesis and subsequent least-squares refinement. The Ir, P, F, N, O, and C atoms were included in the refinement with anisotropic thermal parameters. Hydrogen atoms were placed in calculated positions (d(C−H) = 0.96 Å, d(O−H) = 0.85 Å) with fixed ($U = 0.08$ Å^2) contributions. The CH_2Cl_2 molecules were found to be disordered giving rise to high thermal parameters for all solvent atoms [C(46), C(47), and all Cl atoms]. Then, only their isotropic thermal parameters were refined. The final model converged to $R = 0.070$ and $R' = 0.082$. The final difference Fourier map showed a residual of 1.57 e/Å^3 near Ir (0.89 Å).

Results

Synthesis and Characterization. The novel series of HL-X ligands (X = Cl, Me, COOH) has been prepared by a classical Kröhnke synthesis[20a,b] from the appropriate enone and *N*-phenacylpyridinium bromide in the presence of a large excess of ammonium acetate (Scheme 1, route *a*). Alternatively,[14] the ligand hpbpy (X = OH) has been prepared by a similar synthetic approach via the commercially available 4-hydroxychalcone and *N*-(2-pyridacyl)pyridinium iodide (Scheme 1, route *b*). The latter dienophile has been also used in the preparation of the ligand 4′-(4-tolyl)-2,2′:6′,2″-terpyridine (ttpy) (Scheme 1, route *c*). This method led to a better yield of ttpy than that reported in the literature.[21] Mixed-ligand iridium(III) monomers of the type $[Ir(NC)_2(NN)]^+$ (where NC is an ortho-metalating ligand and NN a neutral, bpy-like chelating ligand) have usually been prepared by bridge-splitting reactions of the appropriate ortho-metalated dimer $[Ir(NC)_2Cl]_2$ with the chelating NN ligand,[5−9] a procedure adapted from the early method employed by Nonoyama[22] for the preparation of $[Rh(bq)_2(bpy)]^+$ (bq = metalated benzo[*h*]-quinoline, bpy = 2,2′-bipyridine). Since previously tested reaction conditions were very different from each other (ranging from room-temperature reactions to reflux in high-boiling solvents), we made several attempts before finding a successful method. Whereas our HL-X ligands failed to react with $[Ir(ppy)_2Cl]_2$ in both a refluxing dichloromethane solution and a refluxing dichloromethane−toluene mixture, pure $[Ir(ppy)_2(HL\text{-}X)]^+$ species (HL-X = hpbpy (**1**), clpbpy (**2**), tpbpy (**3**), and cpbpy (**4**)) were obtained in high yield when the reaction was carried out in refluxing dichloromethane-methanol. The related complex $[Ir(ppy)_2(ttpy)]^+$ (**5**) was prepared in a similar way in view of its use as model compound in photophysical studies. All the cationic complexes **1**−**5**, obtained as the hexafluorophosphate salts, are very soluble in acetonitrile and their solutions remain stable in air for several weeks.

Complexes **1**−**4** were characterized by IR and ^{1}H NMR spectroscopies. The latter technique proved to be more informative with respect to the possibility of ascertain the presence of a single isomer of low symmetry. Although inconclusive because of the large number of unassigned resonances, the NMR evidence pointed to the formation of monomeric species with dissimilar ppy ligands. On average protons of metalated ppy ligands in **1**−**4** experienced larger shielding effects if compared to the parent dimer $[Ir(ppy)_2Cl]_2$.[15] On the basis of integration, *J* values, and homonuclear decoupling experiments, three sets of signals were tentatively assigned to the protons of aromatic rings A, B, and D of the HL-X ligand (**I**). The NMR data for

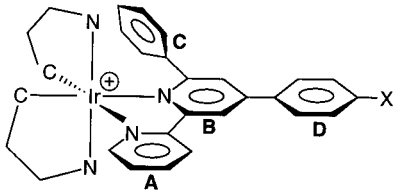

I

complex **5** also confirmed that the complex belongs to the same isostructural series as **1**−**4**, with the potentially tridentate ttpy ligand bound only through two nitrogen donors in a chelating fashion.

Definitive structural assignment relied on a diffractometric study on complex **4** (vide infra). This study allowed two conclusions to be reached. First, no metalation of the phenyl ring (C-ring) of the HL-X ligand had occurred under the experimental conditions. Furthermore, the metalated ppy ligands in these monomeric complexes mantained their mutual cisoid arrangement of the Ir−C bonds, a distinctive structural feature of the dimeric precursor.[23]

Crystal Structure of $[Ir(ppy)_2(cpbpy)][PF_6]$ (4). The crystal structure of complex **4** consists of discrete $[Ir(ppy)_2(cpbpy)]^+$ cations and $[PF_6]^-$ anions with no interionic contacts. The complex crystallizes along with two molecules of solvent of crystallization, which are readily lost when the crystals are exposed to air. Positional parameters, temperature factors, and relevant bond distances and angles are given in Tables 2 and 3. A perspective view of the complex cation of **4** is shown in Figure 1.

The iridium atom is coordinated in a distorted octahedron to four nitrogen and two carbon atoms. The coordination geometry of the ppy ligands around the metal ion is such that the metal−carbon bonds are in a mutual cis orientation. Due to the strong trans influence of the metalated carbon atoms, the Ir−N(cpbpy) distances appear to be significantly longer than the Ir−N(ppy) bond lengths, in agreement with what it is usually observed for related compounds.[6a,23−25] The Ir−C bond distances of 1.992-(12) and 2.035(15) Å are within the range observed for the corresponding distance in Ir(III) CN-chelates with similar geometry and ligand environments.[6a,9b,23−25] The bite angles of the ppy ligands (80.3(5) and 79.6(6)°) lie in the same range as observed before.[6a,9b,23] On the other hand, the bite angle value of the cpbpy ligand (75.2(4)°) is slightly smaller than those reported earlier for Ir(III)-bpy fragments.[26−28]

(18) *SHELXTL PLUS*, Version 4.21; Siemens Analytical X-ray Instruments Inc.: Madison, WI, 1990.
(19) North, A. C. T.; Phillips, D. C. *Acta Crystallogr., Sect. A* **1968**, *24*, 351.
(20) (a) Kröhnke, F. *Synthesis* **1976**, 1. (b) The ligand clpbpy has been recently reported to afford a cyclometalated dinuclear Pt(II) complex, but no details of characterization were given. See, Wu, L.-Z.; Cheung, T.-C.; Che, C.-M.; Cheung, K.-K.; Lam, M. H. W. *Chem. Commun.* **1998**, 1127.
(21) Spahni, W.; Calzaferri, G. *Helv. Chim. Acta* **1984**, *67*, 450.
(22) Nonoyama, M. *J. Organomet. Chem.* **1974**, *82*, 271.
(23) Garces, F. O.; Dedeian, K.; Keder, N. L.; Watts, R. J. *Acta Crystallogr.* **1993**, *C49*, 1117.
(24) Nord, G.; Hazell, A. C.; Hazell, R. G.; Farver, O. *Inorg. Chem.*, **1983**, *22*, 3429.
(25) Urban, R.; Kramer, R.; Shahram, M.; Polborn, K.; Wagner, B.; Beck, W. *J. Organomet. Chem.* **1996**, *517*, 191.
(26) Hazell, A. C.; Hazell, R. G. *Acta Crystallogr.* **1984**, *C40*, 806.
(27) Alexander, B. D.; Johnson, B. J.; Johnson, S. M.; Boyle, P. D.; Kann, N. C.; Mueting, A. M.; Pignolet, L. H. *Inorg. Chem.* **1987**, *26*, 3506.
(28) Albano, V. G.; Bellon, P. L.; Sansoni, M. *Inorg. Chem.* **1969**, *8*, 298.

The central and distal pyridine rings of the cpbpy ligand are almost coplanar (dihedral angle 7°), while the rotationally free 6′-phenyl ring is significantly tilted (dihedral angle 73°) with respect to the central pyridine ring. Moreover, the 6′-phenyl ring is nearly parallel to one metalated 2-phenylpyridine ligand showing dihedral angles of 11.7(4) and 16.0(5)° with respect to the mean planes through the aromatic ring C(40)/C(45) (plane 1) and the pyridine ring N(4)/C(39) (plane 2), respectively. A heterogeneous stack,[29] approximately along the *x* axis, is formed by the 6′-phenyl ring and plane 1. While the aromatic centroid distance is 3.51 Å, the interplanar distance within the stack is 3.24 Å with an offset along the stack of 2.82 Å. Tilt of the 4′-phenyl ring with respect to the central pyridine ring of the cpbpy ligand (diehedral angle 29°) is also noted.

In the crystal packing the carboxyl groups of the coordinated cpbpy ligand of neighboring cations are linked through pairs of hydrogen bonds, affording an eight-membered ring (an $R_2^2(8)$ ring in the graph-set notation[30]). Such a structural feature is typical for assemblies formed from carboxylic acid synthons[31−33] and it has been often observed in metal complexes containing a single COOH group.[34,35] These double hydrogen bridges connect crystallographically equivalent cations related by a center of inversion (Figure 2).The carboxyl dimer is sandwiched between two pyridine rings equally spaced approximately along the *y* axis. The dihedral angle between the mean planes through the eight-membered ring and the pyridine ring is 40° with an interplanar distance of 3.52 Å.

Redox Data, Electronic Spectroscopy, and Photophysics. All the complexes exhibit an irreversible oxidation process between +1.15 and +1.20 V vs SCE and a reversible reduction process between −1.30 and −1.40 V, followed by an irreversible reduction at about −1.90 V. The absorption spectra are dominated by a strong band in the UV region (λ_{max} at about 270 nm, ϵ in the range 10^4-10^5 M^{-1} cm^{-1}) and show less intense absorption features at longer wavelengths. All the complexes are luminescent both at room temperature in fluid acetonitrile solution and at 77 K in a rigid matrix. The luminescence spectra are broad, but the vibrational structure is visible in the shoulders of the red tail of the main band, expecially at 77 K. Luminescence decays are strictly monoexponential and are in the microsecond time scale at 77 K and 1 order of magnitude shorter at 298 K. Table 4 collects the redox data while the spectroscopic and photophysical data are gathered in Table 5. The absorption and luminescence spectra of **1** and **5** are shown in Figures 3 and 4, respectively.

Discussion

The spectroscopic and redox behavior of transition metal complexes and of organometallic compounds are usually discussed with the assumption that the ground state, as well as the excited and redox states involved to explain the observed properties, can be described by a localized molecular orbital configuration.[2b,36] Within such an assumption, the various

Table 2. Atomic Coordinates ($\times 10^4$) and Equivalent Isotropic Displacement Coefficients ($Å^2 \times 10^3$) for $[Ir(ppy)_2(cpbpy)]PF_6 \cdot 2CH_2Cl_2$ (**4**)

atom	*x*	*y*	*z*	*U*(eq)
Ir	2055(1)	1562(1)	2916(1)	37(1)
N(1)	636(9)	1311(3)	1572(6)	40(4)
N(2)	3032(9)	1114(4)	2288(7)	43(4)
N(3)	1799(9)	1001(3)	3717(7)	39(4)
N(4)	2320(10)	2184(4)	2297(8)	56(4)
O(1)	−5058(11)	57(4)	−3868(7)	79(5)
O(2)	−3551(10)	201(6)	−4396(8)	111(6)
C(1)	1085(11)	1020(5)	1041(8)	47(4)
C(2)	336(12)	824(4)	230(8)	47(5)
C(3)	−882(12)	905(5)	−102(9)	51(5)
C(4)	−1357(12)	1173(5)	404(8)	52(5)
C(5)	−583(12)	1375(5)	1275(9)	48(5)
C(6)	2445(12)	929(4)	1413(8)	46(5)
C(7)	3071(13)	684(5)	951(10)	60(6)
C(8)	4250(14)	610(5)	1311(11)	67(6)
C(9)	4917(12)	771(5)	2232(10)	57(5)
C(10)	4280(11)	1017(5)	2679(9)	52(5)
C(11)	−1189(12)	1697(5)	1747(10)	48(5)
C(12)	−1963(16)	1511(7)	2129(11)	80(9)
C(13)	−2607(17)	1787(12)	2557(16)	117(12)
C(14)	−2521(20)	2304(9)	2537(18)	107(11)
C(15)	−1749(21)	2481(8)	2050(15)	106(10)
C(16)	−1122(15)	2207(6)	1694(10)	71(6)
C(17)	−1660(11)	704(5)	−1046(9)	52(5)
C(18)	−1190(14)	625(7)	−1740(11)	82(7)
C(19)	−1974(13)	450(8)	−2655(12)	86(8)
C(20)	−3190(14)	375(5)	−2798(10)	61(6)
C(21)	−3681(14)	440(5)	−2090(10)	64(6)
C(22)	−2930(14)	605(6)	−1242(10)	66(6)
C(23)	−3960(14)	190(5)	−3740(9)	59(5)
C(24)	2604(11)	980(4)	4612(8)	45(4)
C(25)	2425(14)	677(5)	5244(11)	62(6)
C(26)	1439(16)	362(6)	4969(11)	75(7)
C(27)	675(16)	359(6)	4071(12)	75(7)
C(28)	878(13)	695(5)	3442(10)	59(6)
C(29)	3622(12)	1341(5)	4823(8)	50(5)
C(30)	4626(14)	1347(6)	5645(10)	64(6)
C(31)	5536(16)	1678(6)	5759(12)	70(7)
C(32)	5455(13)	2014(5)	5093(11)	62(6)
C(33)	4472(14)	1993(5)	4279(10)	61(6)
C(34)	3506(12)	1662(5)	4082(9)	50(5)
C(35)	1971(13)	2595(5)	2589(10)	55(5)
C(36)	2137(19)	3039(5)	2235(12)	83(8)
C(37)	2656(18)	3058(7)	1529(12)	85(9)
C(38)	3049(19)	2640(7)	1278(15)	96(10)
C(39)	2838(13)	2220(6)	1631(10)	57(6)
C(40)	1348(13)	2514(4)	3293(10)	52(5)
C(41)	998(17)	2911(5)	3736(12)	75(7)
C(42)	365(18)	2799(7)	4329(12)	80(8)
C(43)	167(16)	2329(7)	4540(10)	75(7)
C(44)	560(13)	1958(5)	4104(9)	57(5)
C(45)	1183(12)	2042(5)	3477(9)	48(5)
P	2396(4)	327(2)	8122(3)	83(2)
F(1)	2201(12)	796(5)	8622(8)	120(6)
F(2)	1289(16)	464(7)	7274(11)	175(9)
F(3)	3593(15)	199(8)	8980(11)	187(10)
F(4)	2609(18)	−107(8)	7555(14)	208(11)
F(5)	1547(20)	76(6)	8543(18)	211(16)
F(6)	3118(20)	639(10)	7656(15)	223(14)
C(46)	5028(55)	1549(20)	9265(23)	461(64)
Cl(1)	5257(11)	1607(3)	10321(8)	174(4)
Cl(2)	5640(9)	1800(3)	8627(7)	172(3)
C(47)	8036(37)	1312(14)	5076(26)	205(15)
Cl(3)	9349(16)	1333(6)	6001(11)	264(6)
Cl(4)	7826(14)	921(5)	4291(11)	246(5)

(29) André, I.; Foces-Foces, C.; Cano, F. H.; Martinez-Ripoll, M. *Acta Crystallogr.* **1997**, *B53*, 984.
(30) (a) Etter, M. C. *Acc. Chem. Res.* **1990**, *23*, 120. (b) Etter, M. C.; MacDonald, J. C.; Bernstein, J. *Acta Crystallogr.* **1990**, *B46*, 256.
(31) Leiserowitz, L. *Acta Crystallogr.* **1976**, *B32*, 775.
(32) (a) Desiraju, G. R. *Angew. Chem., Int. Ed. Engl.* **1995**, *34*, 2311. (b) Desiraju, G. R. *Acc. Chem. Res.* **1996**, *29*, 441.
(33) Allen, F. H.; Raithby, P. R.; Shields, P.; Taylor, R. *Chem. Commun.* **1998**, 1043.
(34) Braga, D.; Grepioni, F.; Sabatino, P.; Desiraju, G. R. *Organometallics* **1994**, *13*, 3532.
(35) Schneider, W.; Bauer, A.; Schmidbaur, H. *Organometallics* **1996**, *15*, 5445.
(36) De Armond, M. K.; Carlin, C. M. *Coord. Chem. Rev.* **1981**, *36*, 325.

Table 3. Selected Bond Lengths (Å) and Angles (deg) for $[Ir(ppy)_2(cpbpy)]PF_6 \cdot 2CH_2Cl_2$ (**4**)

Ir−N(1)	2.240(8)	Ir−N(2)	2.125(12)
Ir−N(3)	2.064(10)	Ir−N(4)	2.040(13)
Ir−C(34)	1.992(12)	Ir−C(45)	2.035(15)
N(1)−C(1)	1.370(18)	N(2)−C(6)	1.365(15)
C(1)−C(6)	1.501(17)	N(3)−C(24)	1.357(13)
C(24)−C(29)	1.495(18)	C(29)−C(34)	1.407(19)
N(4)−C(35)	1.337(20)	C(35)−C(40)	1.508(24)
C(40)−C(45)	1.366(18)	C(20)−C(23)	1.490(18)
O(1)−C(23)	1.275(20)	O(2)−C(23)	1.249(22)
N(1)−Ir−N(2)	75.2(4)	N(1)−Ir−N(3)	95.3(3)
N(2)−Ir−N(3)	92.1(4)	N(1)−Ir−N(4)	91.3(4)
N(2)−Ir−N(4)	95.4(5)	N(3)−Ir−N(4)	171.0(4)
N(1)−Ir−C(34)	168.0(5)	N(2)−Ir−C(34)	93.7(5)
N(3)−Ir−C(34)	80.3(5)	N(4)−Ir−C(34)	94.4(5)
N(1)−Ir−C(45)	105.8(4)	N(2)−Ir−C(45)	174.9(5)
N(3)−Ir−C(45)	92.8(5)	N(4)−Ir−C(45)	79.6(6)
C(34)−Ir−C(45)	85.7(5)		

spectroscopic transitions are classified as metal-centered (MC), ligand-centered (LC), or charge-transfer (either metal-to-ligand, MLCT, or ligand-to-metal, LMCT), and the oxidation and reduction processes are classified as metal- or ligand-centered. This simplified picture is of course less applicable to organometallic compounds, where a large degree of covalency exists in metal−ligand bonds.[2d] Furthermore, very recently other types of orbitals (and states) have been invoked to elucidate the spectroscopic and electrochemical properties of metal compounds with strong electron donor ligands. For example, a covalent metal−C^- σ-bonding (or metal-Si^- σ-bonding) orbital has been identified as the orbital involved in the oxidation process and the lowest-lying charge-transfer excited state in Ir(III) and Rh(III)-cyclometalated compounds.[5e,8b] In particular, Kirsh-De Mesmaeker and co-workers[8b] argued that the lowest energy excited state of $[Ir(ppy)_2TAP]^+$, $[Rh(ppy)_2TAP]^+$ and $[Rh(ppy)_2HAT]^+$ (TAP = 1,4,5,8-tetraazaphenanthrene; HAT = 1,4,5,8,9,12-hexaazatriphenylene) would involve a transition from such a σ-bond orbital to a π^* orbital of the polypyridine ligand (σ-bond to ligand charge transfer, SBLCT). It can be noted that this excited state may be considered as a particular case of ligand-to-ligand charge-transfer (LLCT) state, following the definition given by Vogler and co-workers.[37]

Redox Behavior. As pointed out above, the oxidation processes of Ir(III) cyclometalated compounds have been attributed to metal-centered orbitals and to covalent metal−C^- σ-bonding (or metal−Si^- σ-bonding) orbitals. It was found that iridium-centered oxidation is usually reversible, while oxidations involving HOMOs with pronounced contributions from σ-bond orbitals are irreversible. Because of the irreversible nature of the oxidation processes exhibited by the complexes studied here, we assign such oxidations to orbitals which receive a strong contribution from Ir−C^- σ-bond orbitals. A further argument supporting this assignment originates from the comparison of the oxidation data reported in Table 4 with those of $[Ir(ppy)_2(dpt\text{-}NH_2)]^+$ (dpt-NH_2 = 4-amino-3,5-bis(2-pyridyl)-4*H*-1,2,4-triazole).[7] This latter compound undergoes a reversible, metal-centered oxidation at 1.23 V vs SCE, under the same experimental conditions used for **1**−**5**. If one considers the greater acceptor ability of the polypyridine ligands which are present in **1**−**5** compared with dpt-NH_2, the metal-centered orbital in **1**−**5** should be stabilized with respect to that of $[Ir(ppy)_2(dpt\text{-}NH_2)]^+$, and the metal-centered oxidation should move to more positive potentials. The experimental observation (Table 4) indicates that this is not the case, suggesting that metal-centered assignment for the oxidation processes of **1**−**5** is hardly acceptable. Stabilization of the Ir d_π orbital decreases the energy gap between such orbital and the σ-bond orbital, so inducing a substantial contribution of the σ-bond orbital to the HOMO in **1**−**5**. Similar behavior has been reported for the complex $[Ir(ppy)_2HAT]^+$.[8b]

Comparison of the data of **1**−**5** with those for $[Ir(ppy)_2(bpy)]^+$ (studied in DMF, vs ferrocene)[5c] is instructive for assigning the reduction processes. $[Ir(ppy)_2(bpy)]^+$ undergoes a first reduction process at −1.77 V vs ferrocene, assigned to the bpy ligand, and a second one at −2.42 V, assigned to a ppy ligand. On the basis of these data as well as of the redox data reported for other Ir(III) species,[2d] we assign the first reduction of **1**−**5** to the noncyclometalating polypyridine ligand(s) and the second process to a metalated ppy ligand. The similarity of the redox potentials of **1**−**5** indicates that the para substituents on the 4′-phenyl ring have only a slight influence on the redox behavior of the complexes.

Absorption Spectra. The intense band peaking at about 270 nm which is present in all the absorption spectra of the complexes (Table 5, Figures 3 and 4) is typical of cyclometalated phenylpyridine compounds,[2d] and it is therefore assigned to spin-allowed LC transitions centered on these ligands. Bipyridine-centered transitions in transition metal complexes usually exhibit an absorption maximum in the region 270−300 nm,[2d] so we can safely attribute the shoulder at about 290 nm (Figures 3 and 4) to these transitions. In **1** this shoulder is shifted to lower energy (Table 5) most probably because of superimposed charge-transfer transitions internal to the hpbpy ligand. On the basis of the extinction coefficients, the energy, and literature data,[2d,5−9] the shoulder around 370 nm which is present in all the compounds studied here (Table 5, Figures 3 and 4) is assigned to spin-allowed charge-transfer transitions, although it is not easy to discriminate between pure MLCT and SBLCT transitions. It is interesting to note that **5** (Figure 4) exhibits additional absorption features at 350 and 415 nm, not shown by **1**−**4**. These features can be ascribed to the presence of the nonchelating pyridyl ring, but their detailed assignment is not clear.

Finally, the absorption spectra of all the complexes show a long tail which extends toward the red, exhibiting a shoulder at 470 nm (Table 5, Figures 3 and 4). Because of the energy and the low extinction coefficient, this low-energy band is assigned to spin-forbidden CT transitions which steal intensity from the relative spin-allowed transitions because of the strong spin−orbit coupling induced by the heavy metal ion.

Similarly to previous observations for the redox properties, the remote substituents on the 4′-phenyl ring have only slight effects on the absorption spectra of the compounds, showing that the chromophore is essentially unperturbed by their presence at least as far as the absorption properties are concerned. Such results are in fair agreement with those reported for the properties of different metal-based chromophores by remote substituents.[38]

Luminescence Properties. Both MLCT and SBLCT luminescence have been reported for Ir(III) cyclometalated compounds.[5−9] To discriminate between the two types of emission is not an easy task from an experimental viewpoint. The main difference is probably related to the fact that SBLCT excited states are usually more distorted than MLCT states with respect to the ground state. So SBLCT emitters exhibit luminescence

(37) Vogler, A. In *Photoinduced Electron Transfer (Part D)*; Fox, M. A., Chanon, M., Eds.; Elsevier: New York, 1988; p 179.

(38) Thummel, R. P.; Hedge, V.; Jahng, Y. *Inorg. Chem.* **1988**, *28*, 3264.

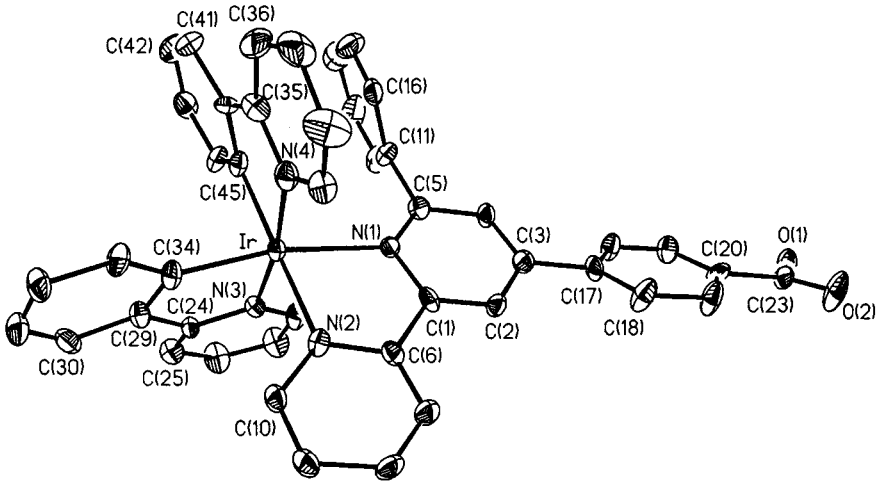

Figure 1. Diagram of the molecular structure of the cation of $[Ir(ppy)_2(cpbpy)][PF_6]$ (**4**) with atomic numbering and thermal ellipsoids (50% probability level). Hydrogen atoms are omitted for clarity.

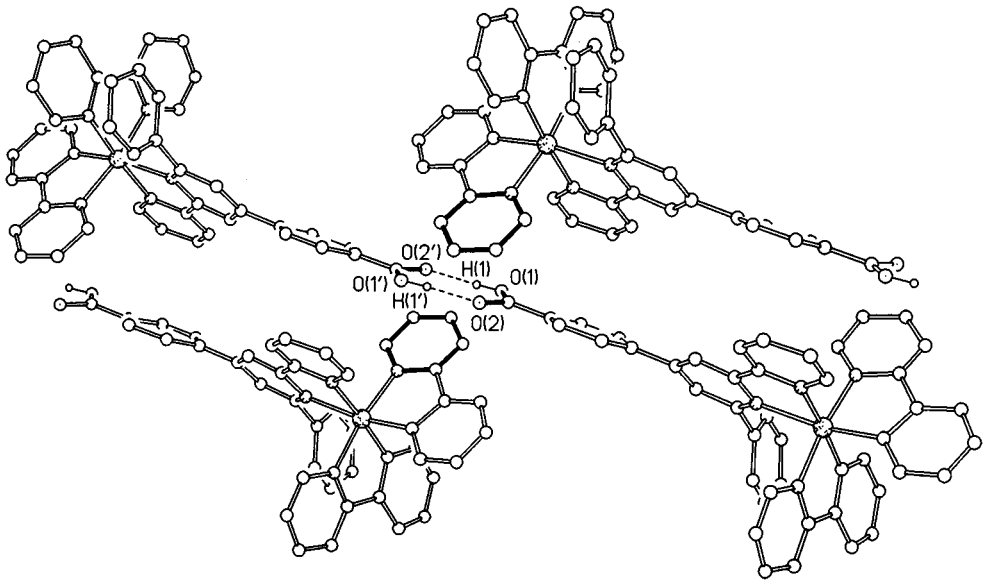

Figure 2. Crystal packing for $[Ir(ppy)_2(cpbpy)][PF_6]$ (**4**) showing the double hydrogen bridges between the carboxylic acid groups. Aromatic hydrogen atoms omitted for clarity. Hydrogen bonding parameters: O(1)−H(1) = 0.85 Å, H(1)−O(2a) = 1.83 Å, O(1)−O(2a) = 2.67(1) Å, O(1)−H(1)−O(2a) = 169.9°.

Table 4. Half-Wave Potentials in Argon-Purged Acetonitrile Solution, 298 K

compound	$E_{1/2}$(ox), V vs SCE	$E_{1/2}$(red), V vs SCE
1 $[Ir(ppy)_2(hpbpy)]^+$	+1.18[a]	−1.40; −1.90[a]
2 $[Ir(ppy)_2(clpbpy)]^+$	+1.19[a]	−1.33; −1.84[a]
3 $[Ir(ppy)_2(tpbpy)]^+$	+1.18[a]	−1.37; −1.85[a]
4 $[Ir(ppy)_2(cpbpy)]^+$	+1.16[a]	−1.36; −1.89[a]
5 $[Ir(ppy)_2(ttpy)]^+$	+1.20[a]	−1.36; −1.90[a]

[a] Irreversible process. In this case, the value reported is the dpv peak.

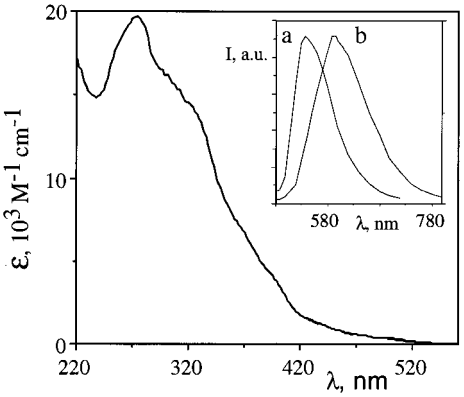

Figure 3. Absorption spectrum of complex **1** in acetonitrile fluid solution at room temperature. The inset shows the uncorrected emission spectra for the same compound (a) at 77 K in MeOH/EtOH 4:1 (v/v) mixture and (b) at room temperature in acetonitrile. The corrected emission maxima are given in Table 5.

spectra having a larger half-width and an increased blue shift with respect to pure MLCT emitters on passing from a fluid solution at 298 K to rigid matrixes at 77 K. Based on the evidence that in **1**−**5** the shift is typically 2400 cm^{-1} (very close to the value of 2200 cm^{-1} exhibited by $[Ir(ppy)_2(dpt\text{-}NH_2)]^+$, a typical MLCT emitter[7]) and the half-width of the emission spectra at room temperature is around 1700 cm^{-1} (close to the half-widths of the MLCT emission spectra of Ru(II) and Os(II) polypyridine complexes,[2] usually in the range 1500−2000 cm^{-1}), it seems that the luminescence of the new complexes is dominated by triplet MLCT levels. Anyway these levels have also a partial SBLCT character, as suggested by the redox results.

Table 5. Absorption and Luminescence Properties; Data Are in Acetonitrile Deoxygenated Solution at Room Temperature, Unless Otherwise Noted

compound	absorbance λ_{max}, nm (ϵ, M^{-1} cm^{-1})	luminescence, 298 K λ_{max}, nm	τ, ns	Φ	luminescence, 77 K[a] λ_{max}, nm	τ, μs	k_r, s^{-1} [b]	k_{nr}[c]
1 $[Ir(ppy)_2(hpbpy)]^+$	270 (20000) 320 sh (15100) 375 (4400) 475 sh (370)	620	180	0.032	545	3.93	1.78×10^5	5.53×10^6
2 $[Ir(ppy)_2(clpbpy)]^+$	270 (19900) 290 sh (17100) 385 (2700) 475 sh (350)	645	135	0.023	555	3.48	1.70×10^5	7.24×10^6
3 $[Ir(ppy)_2(tpbpy)]^+$	270 (20270) 290 sh (17100) 380 sh (3100) 475 sh (330)	630	160	0.031	550	3.64	1.94×10^5	6.06×10^6
4 $[Ir(ppy)_2(cpbpy)]^+$	268 (21400) 295 sh (16000) 382 (3000) 475 sh (380)	660	125	0.017	565	3.26	1.36×10^5	7.86×10^6
5 $[Ir(ppy)_2(ttpy)]^+$	266 (19200) 320 sh (12000) 370 (3000) 475 sh (330)	625	70	0.017	560	3.87	2.43×10^5	1.40×10^7

[a] In MeOH/EtOH 4:1 (v/v). [b] Rate constant of radiative decay at 298 K, calculated by $k_r = \Phi/\tau$. [c] Rate constant of radiationless decay at 298 K, calculated by $k_{nr} = 1/\tau - k_r$.

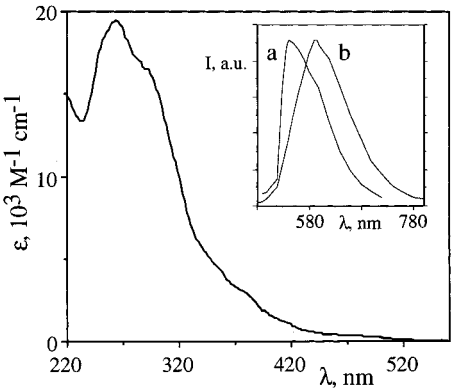

Figure 4. Absorption spectrum of complex **5** in acetonitrile fluid solution at room temperature. The inset shows the uncorrected emission spectra for the same compound (a) at 77 K in MeOH/EtOH 4:1 (v/v) mixture and (b) at room temperature in acetonitrile. The corrected emission maxima are given in Table 5.

Leaving aside **5**, the luminescence energies, both at 77 and at 298 K, increase along the series in the order **4** < **2** < **3** < **1**. This can be explained looking at the acceptor abilities of the remote substituents on the 4′-phenyl ring, which are expected to decrease going from acceptor carboxyl and chloride groups to donor methyl and hydroxyl substituents. The presence of better acceptor substituents make easier reduction of the coordinating bpy subunit of the ligands, so moving the MLCT state to lower energies. It is interesting to note that for **1**−**4** luminescence lifetimes at 77 K are shortened as the excited-state energy is lowered. In particular, there is a linear relationship (Figure 5) between ln $(1/\tau)$ and the 77 K emission maxima of the complexes (which are approximately equivalent to the energies of the emitting states). In other words, assuming that $1/\tau$ is equivalent to the rate constant for radiationless decay, k_{nr}, the series of complexes **1**−**4** obeys the energy gap rule.[39] This rule was previously demonstrated for Ru(II), Os(II), and

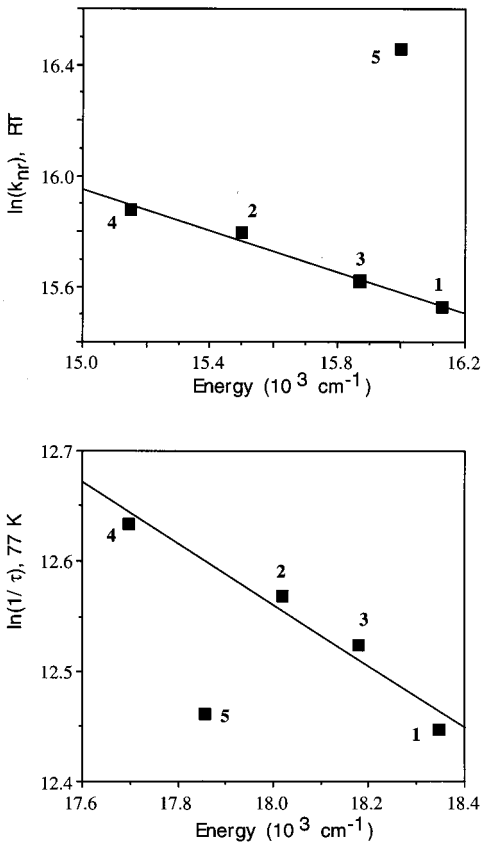

Figure 5. Ln$(1/\tau)$ vs emission energy (E_{em}) at 77 K in rigid matrix (bottom) and ln k_{nr} vs emission energy maxima at 298 K (top) for the studied complexes. The lines shown are the least-squares fit to the data except for complex **5**.

Re(I) MLCT emitters[40] but has not been yet verified for Ir(III) luminophores, although there were no particular reasons to

(39) Siebrand, W. *J. Chem. Phys.* **1967**, *46*, 440.

(40) (a) Caspar, J. V.; Kober, E. M.; Sullivan, B. P.; Meyer, T. J. *J. Am. Chem. Soc.* **1982**, *104*, 630. (b) Caspar, J. V.; Meyer, T. J. *J. Phys. Chem.* **1983**, *87*, 952. (c) Lumpkin, R. S.; Meyer, T. J. *J. Phys. Chem.* **1986**, *90*, 5307. (d) Claude, J. P.; Meyer, T. J. *J. Phys. Chem.* **1995**, *99*, 51.

expect different results. The essence of the energy gap rule is that the promoting modes driving the radiationless decay are identical in the series of luminophores and the Franck−Condon factor of the transition depends only on the energy gap between the states. The fact that the law is obeyed by all the complexes studied here except **5** suggests that the excited state of **5** is different with respect to those of **1**−**4** as far as its deactivation dynamics are concerned. This means that the replacement of the 6′-phenyl ring of HL-X in **1**−**4** with a pyridine ring in **5** perturbs the luminescent ^{3}MLCT level leading to modification either of (i) the electronic coupling between ground and excited states, or (ii) the vibrational energy of the promoting modes, or (iii) the excitation state distortion with respect to the ground state. The presence of perturbations is also suggested by the absorption spectrum of **5**, different in the MLCT region with respect to **1**−**4** (see above). It has been proposed that excited-state dynamics may be affected even in the absence of any sizable effects on the energy level of the excited states,[41] so it is not surprising that the redox and (partially) the absorption data are not influenced to the same extent.

The linear relationship between ln k_{nr} and the emission energy at 298 K yields a slope of -2.98 eV^{-1} and an intercept of 21.534 (correlation coefficient, 0.983), whereas a slope of -2.25 eV^{-1} is obtained for the 77 K data. The values of the slopes are significantly smaller than those of polypyridine complexes containing other metals (e.g.; Os(II) and Ru(II) bipyridine complexes exhibit slopes in the range -7.00 and -8.00 eV^{-1} in acetonitrile[40a] and tricarbonyl(bipyridine) Re(I) complexes exhibit slopes in the range -9.00 and -12.00 eV^{-1} in acetonitrile[40b,42]).

The milder dependence of the k_{nr} on the excited-state energy of the complexes studied here with respect to other MLCT emitters suggests significant differences in the vibronic wave functions involved in the deactivation processes. Such differences could arise, for example, from different dominating accepting modes and/or from different anharmonicity character in the vibronic states involved. To investigate in detail this point different types of experiments and calculations are needed, but they are out of the aim of this paper.

Conclusion

We synthesized a series of functionalized polypyridine HL-X ligands in order to prepare new Ir(III) cyclometalated compounds and to obtain further insights into the photophysical properties of such a class of compounds. All the synthesized metal complexes exhibit oxidation mainly centered on an orbital derived from an Ir−C$^-$ σ-bond and ligand-centered reduction processes. They are also luminescent from ^{3}MLCT levels both at 77 K in a rigid matrix and at 298 K in fluid solution.

The remote substituents on the rotationally free 4′-phenyl ring of HL-X do not significantly perturb the redox-active chromophore. However, while the redox and absorption properties are more or less insensitive to the remote substituents, fine-tuning of the luminescence properties is observed. Because of the high luminescence quantum yield and of the presence of the X functionalities in the periphery of the polypyridine ligand framework, the complexes reported here may be considered as promising building blocks for light- and redox-active multicomponent, supramolecular systems.

Acknowledgment. Financial support from the italian Ministero dell'Università e della Ricerca Scientifica e Tecnologica (MURST) and Consiglio Nazionale delle Ricerche (CNR) is gratefully acknowledged.

Supporting Information Available: Full distance and angle listings, hydrogen atom coordinates, and anisotropic temperature factors for compound **4**. This material is available free of charge via the Internet at http://pubs.acs.org.

IC981308I

(41) Guglielmo, G.; Ricevuto, V.; Giannetto, A.; Campagna, S. *Gazz. Chim. Ital.* **1989**, *119*, 457.
(42) Baiano, J. A.; Murphy, W. R., Jr. *Inorg. Chem.* **1991**, *30*, 4594.